Optics Communications 402 (2017) 216–220

Contents lists available at ScienceDirect

Optics Communications

journal homepage: www.elsevier.com/locate/optcom

Localized surface plasmon resonance properties of Ag nanorod arrays on graphene-coated Au substrate

Haiwei Mu [a], Jingwei Lv [a], Chao Liu [a,*], Tao Sun [b], Paul K. Chu [c], Jingping Zhang [d]

[a] School of Electronics Science, Northeast Petroleum University, Daqing 163318, PR China
[b] Institute of Microelectronics, Agency for Science, Technology and Research (A*STAR), Singapore, 117685, Singapore
[c] Department of Physics and Materials Science, City University of Hong Kong, Tat Chee Avenue, Kowloon, Hong Kong, China
[d] School of Electrical Engineering and Information, Northeast Petroleum University, Daqing 163318, PR China

ARTICLE INFO

Keywords:
LSPR
DDA
SNR/graphene/Au substrate

ABSTRACT

Localized surface plasmon resonance (LSPR) on silver nanorod (SNR) arrays deposited on a graphene-coated Au substrate is investigated by the discrete dipole approximation (DDA) method. The resonance peaks in the extinction spectra of the SNR/graphene/Au structure show significantly different profiles as SNR height, and refractive index of the surrounding medium are varied gradually. Numerical simulation reveals that the shifts in the resonance peaks arise from hybridization of multiple plasmon modes as a result of coupling between the SNR arrays and graphene-coated Au substrate. Moreover, the LSPR modes blue-shifts from 800 nm to 700 nm when the thickness of the graphene layer in the metal nanoparticle (NP) - graphene hybrid nanostructure increases from 1 nm to 5 nm, which attribute to charge transfer between the graphene layer and SNR arrays. The results provide insights into metal NP-graphene hybrid nanostructures which have potential applications in plasmonics.

1. Introduction

Noble metallic nanostructures such as gold (Au) and silver (Ag) have attracted much attention because of their prominent and versatile optical properties based on localized surface plasmon resonance (LSPR) [1–3]. LSPR occurs when the electrons inside metallic nanoparticles collectively oscillate with electromagnetic radiation [4,5]. By appropriately engineering the size, shape, and surrounding medium of the metallic nanostructures, LSPR excitation can generate significantly enhanced local electromagnetic fields which can be exploited in photovoltaics [6], surface-enhanced spectroscopy [7], and chemical and biological sensors [8,9].

Since the plasmonic properties of noble metallic nanostructures depend on their geometries, tailoring the morphology of nanoparticles is one of the popular approaches to suit particular applications. However, deposition of metallic nanoparticles on metallic substrates is a viable means. For example, a two-dimensional (2D) gold nanoparticle array placed above a thin gold substrate generates multiple resonance modes in the extinction spectra [10]. Mock et al. [11] reported that the spectral response was highly sensitive to the particle–substrate separation distance when gold nanoparticles were placed nanometers away from a gold substrate. Chen et al. [12] observed doughnut-shaped patterns in far-field scattering images obtained from gold nanorods and metallic substrates. Since the multiple resonance modes between the metal nanoparticles and metal substrate can modify the plasmonic properties, it is reasonable to believe that the fields confined between the metal nanoparticles and metal substrate should show a more complex phenomenon [13]. Recently, much effort has been made to combine noble metal nanoparticles with graphene through surface plasmons. Graphene has novel properties [14–16] and boasting high physical–chemical stability and relatively low dissipative loss, it is an alternative to metallic plasmonic materials [17,18]. However, there is relatively little information on LSPR on metallic nanostructures with a graphene buffer layer on a metal substrate.

Herein, the discrete dipole approximation (DDA) code is employed to theoretically determine the plasmonic properties of graphene-coated Au substrate decorated with SNR arrays. The effects of the graphene layer thickness, SNR height, and refractive index of the surrounding medium on the LSPR properties of the hybrid nanostructure are studied. The electric field enhancement contour around the SNR/graphene/Au structure is analyzed based on multiple resonance modes.

* Corresponding author.
E-mail address: msm-liu@126.com (C. Liu).

http://dx.doi.org/10.1016/j.optcom.2017.06.002
Received 29 December 2016; Received in revised form 25 May 2017; Accepted 1 June 2017
0030-4018/

2. Theoretical assessment

The numerical approach of DDA is used to calculate the electromagnetic field distribution of the arbitrary structure, shape, and size and the scattering spectra, absorption spectra, and extinction spectra of the nanoparticles are derived. In DDA, the target is measured by a cubic array of N polarizable points [19,20]. Generally, the continuum target can be substituted by discrete dipoles as long as the dipole number N is large enough, whose positions and polarizabilities are denoted as $\mathbf{r}_j$ and α_j^{CM} $(i = 1, 2, \ldots)$. α_j^{CM} can be achieved by

$$\alpha_j^{CM} = \frac{3d^3}{4\pi}\frac{\varepsilon_j - 1}{\varepsilon_j + 2} \tag{1}$$

where d is the interdipole spacing and ε_j is the dielectric function of the target material at location $\mathbf{r}_j$.

Analytical modification in Eq. (1) has been reportedly implemented in DDSCAT, the open source computational code of the DDA method [21]. DDSCAT creates a cubic lattice array of dipoles and assigns to each one a polarizability given by the lattice dispersion relation (LDR):

$$\alpha^{LDR} \approx \frac{\alpha^{CM}}{1 + (\alpha^{CM}/d^3)[(b_1 + m^2 b_2 + m^2 b_3 S)(kd)^2 - (2/3)i(kd)^3]} \tag{2}$$

$$b_1 = -1.891531, \qquad b_2 = 0.1648469,$$

$$b_3 = -1.7700004, \qquad S \equiv \sum_{j=1}^{3}(\hat{\alpha}_j \hat{e}_j)^2 \tag{3}$$

where $\hat{\alpha}$ and $\hat{e}$ are unit vectors defining the incident direction and the polarization state, S, b_1, b_2 and b_3 are the coefficients of the expansion to the third-order in k to incorporate radiation effects.

The polarization vector is generated by the interaction between the arbitrary point dipole and local electric field $\mathbf{E}_j$ so that

$$\mathbf{P}_j = \alpha_j \mathbf{E}_j \tag{4}$$

where α_j is the tensor of polarizability of the point dipole and $\mathbf{r}_j$ is the central position. $\mathbf{E}_j$ consists of the electric field $\mathbf{E}_{inc,j}$ at position j due to the incident plane wave and the electric field stimulated by $(N-1)$ other dipoles is as follows

$$\mathbf{E}_{inc,j} = \mathbf{E}_0 \exp i(\mathbf{k}\cdot\mathbf{r}_j - \omega t) \tag{5}$$

$$\mathbf{E}_j = \mathbf{E}_{inc,j} - \sum_{k\neq j}\mathbf{A}_{jk}\mathbf{P}_k \tag{6}$$

where $-\mathbf{A}_{jk}\mathbf{P}_k$ represent the contribution to the electric field at $\mathbf{r}_j$ that is due to the dipole $\mathbf{P}_k$ at position $\mathbf{r}_k$, including retardation effects. Each element $\mathbf{A}_{jk}$ is a 3×3 matrix

$$\mathbf{A}_{jk} = \frac{\exp(ikr_{jk})}{r_{jk}} \times \left[k^2(\hat{r}_{jk}\hat{r}_{jk} - \mathbf{1}_3) + \frac{ikr_{jk} - 1}{r_{jk}^2}(3\hat{r}_{jk}\hat{r}_{jk} - \mathbf{1}_3)\right], \quad j \neq k \tag{7}$$

where $|\mathbf{k}| \equiv \omega/c, \mathbf{r}_{jk} \equiv \left|\mathbf{r}_j - \mathbf{r}_k\right|, \hat{r}_{jk} \equiv (\mathbf{r}_j - \mathbf{r}_k)/r_{jk}$, and $\mathbf{1}_3$ is the 3×3 identity matrix. Defining $\mathbf{A}_{jj} = \alpha_j^{-1}$ reduces the scattering problem to finding the polarizations $\mathbf{P}_j$ that can be briefly described as a set of $3N$ complex linear vector equations

$$\sum_{k=1}^{N}\mathbf{A}_{jk}\mathbf{P}_k = \mathbf{E}_{inc,j}. \tag{8}$$

Once the polarization $\mathbf{P}_j$ is known, the absorption cross section of the entire grain is

$$C_{abs} = \frac{4\pi k}{|\mathbf{E}_0|^2}\sum_{j=1}^{N}\left\{\mathrm{Im}\left[\mathbf{P}_j \cdot \left(\alpha_j^{-1}\right)^* \mathbf{P}_j^*\right] - \frac{2}{3}k^3\left|\mathbf{P}_j\right|^2\right\}. \tag{9}$$

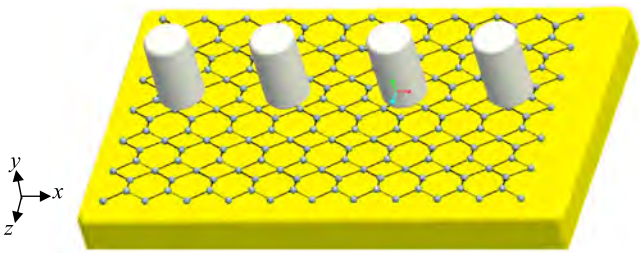

Fig. 1. Schematic illustration of the graphene-coated Au substrate decorated with SNR arrays.

The extinction cross section can be obtained by the optical theorem (7):

$$C_{ext} = \frac{4\pi k}{|\mathbf{E}_0|^2}\sum_{j=1}^{N}\mathrm{Im}\left(\mathbf{E}_{inc,j}^* \cdot \mathbf{P}_j\right). \tag{10}$$

Fig. 1 shows the schematic diagram of the SNR array deposited on the graphene-coated Au substrate. In this simulation, a 1 nm thick graphene is considered to comprise three single-atomic carbon layers. The SNR array has a cylindrical shape 10 nm in diameter and 20 nm tall, and the center-to-center distance between nanorods is maintained at 12 nm. The thicknesses of graphene layer and Au substrate are 1 nm and 50 nm, respectively. The refractive index (n_s) of the surrounding medium is $n_s = 1.41$. The wave vector of the incident light is considered to be linearly polarized with its electric field being oriented along the y axis in the following calculation. The dielectric permittivity of gold and silver used in the calculations is described by the Lorentz–Drude model. The optical constants of bulk silver and gold are obtained from Palik's handbook [20] and SOPRA N&K database [21]. It is noted that the dielectric response of graphene in the visible to near UV range can change dramatically depending on the work function of the metal. In this work, the dielectric response of graphene contacted with metal is calculated based on the density functional theory (DFT) [22–29].

3. Results and discussion

In order to investigate influence of graphene layer thicknesses on LSPR of the hybrid nanostructure, the extinction spectra of the SNRs/graphene/Au nanostructure with different graphene layer thicknesses are plotted in Fig. 2. The refractive index (n_s) of the surrounding medium is set to $n_s = 1.41$ and the thickness of the graphene layers ranges from 1 to 5 nm. Each nanostructure exhibits three resonance modes in the extinction spectra. The resonance mode at $\lambda = 300$ nm has no significant dependence on the thickness of graphene layers, whereas the resonance modes at $\lambda = 643$ nm and $\lambda = 800$ nm blue-shift as the thickness of the graphene layers increases from 1 nm to 5 nm. Specifically, free electrons in the SNRs interact with the electrical charges in the graphene-coated Au substrate, leading to the hybridization of various plasmon modes and giving rise to plasmon shifts [30]. This result shows the resonance mode at $\lambda = 300$ nm of the coupling interaction between the SNR array and graphene-coated Au substrate, which is partially damped by the overlap with the tail of the interband transitions of the Au substrate [31]. Because the LSPR in the SNRs/graphene/Au nanostructure is the convolution of multiple resonance modes, the blue-shift is likely due to different dielectric environments probed on the opposite faces of the nanohybrids when the thickness of graphene layer is varied from 1 to 5 nm. It is also believed that the blue-shift comes from charge transfer between the graphene layer and SNR array. Therefore, the plasmon resonance on the SNRs/graphene/Au nanostructures can be tuned by changing the thickness of the graphene layers.

Plasmon resonances are often categorized into two types: propagating surface plasmon polariton (SPP) waves and localized surface plasmon (LSP) modes, confined to subwavelength metallic objects [32].

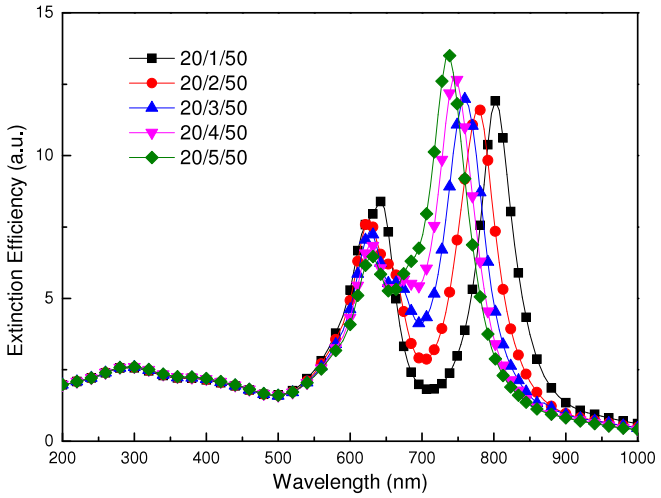

Fig. 2. Extinction spectra of the silver nanorods (SNRs)/graphene/Au nanostructure with different graphene layer thicknesses. (For interpretation of the references to color in this figure legend, the reader is referred to the web version of this article.)

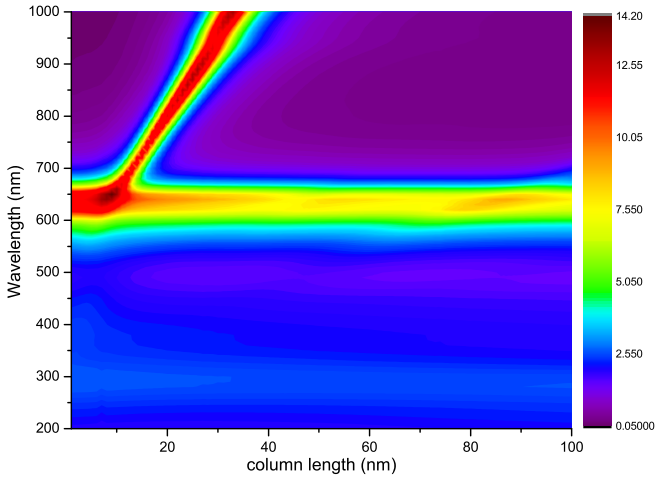

Fig. 3. Extinction spectra of the SNRs/graphene/Au nanostructure with various SNRs heights.

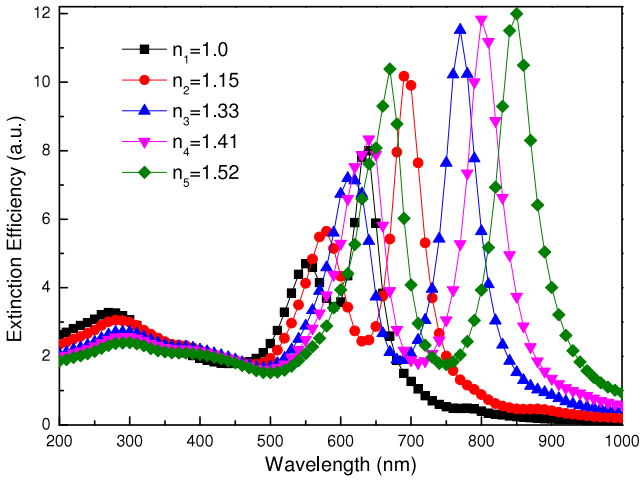

Fig. 4. Extinction spectra of the SNRs/graphene/Au nanostructure as a function of refractive indexes of the surrounding medium. (For interpretation of the references to color in this figure legend, the reader is referred to the web version of this article.)

The plasmon resonance of the SNRs/graphene/Au nanostructures can be visualized as hybridization of multiple plasmon modes. The metallic Au substrate supports SPP mode confined along each of its two interfaces. And in vacuum it is well known that such a nanostructure made of SNR array, which possesses several LSP modes. In the extinction spectrum of the SNRs/graphene/Au nanostructure, three resonances can be seen. The first resonance at 300 nm correspond to the SPP mode on the gold film, and the last two resonances at 643 and 800 nm occur at a very similar wavelength to that of single silver nanorod and correspond to the LSP modes of the silver nanorods.

Fig. 3 displays the extinction spectra of the SNRs/graphene/Au nanostructure with different heights of SNRs. The height of the SNRs is varied from 1 to 100 nm and the interval between nanorods is 1 nm. The hybrid nanostructure shows two extinction bands between 600 and 1000 nm. The lower and higher resonance peaks are attributed to the transverse and longitudinal modes, respectively [33]. With respect to the transverse mode, it only shifts slightly at 630 nm as the height of the SNRs increases and it most likely arises from the cylindrical shape [34]. The longitudinal mode shifts and broadens to larger wavelengths with increasing SNRs height. The incident light is coupled to the LSPR mode of a single Ag nanorod interacting with the closer neighbors leading to the longitudinal mode [35].

The extinction spectra of the SNRs/graphene/Au nanostructure for different refractive indexes of the surrounding medium are shown in Fig. 4. A series of refractive indexes $[n_1, n_2, n_3, n_4, n_5] = [1.0, 1.15, 1.33, 1.41, 1.52]$ are used in the calculation. The red-shift in the longitudinal mode from 630 to 850 nm bears a positive relationship with the refractive index between 1.0 and 1.52. Similarly, the transverse mode red-shifts with increasing refractive index. This variation is due to the change in the refractive index of the surrounding medium around the SNRs/graphene/Au nanostructure, resulting in changes in the resonance condition and location of the resonance modes [36].

Fig. 5 presents the contours of the electric field enhancement of the SNRs/graphene/Au nanostructure at different resonance wavelengths for a surrounding medium with the refractive index of 1.41. Fig. 5(a) shows that the electronic enhancement is mainly distributed on the corners of the graphene-coated gold substrate at 300 nm. Therefore, the light scattered by the SNR array is coupled back to the surface plasmon polariton mode on the graphene-coated gold substrate [37]. The electric field enhancement at 643 nm corresponding to the transverse mode is presented in Fig. 5(b). In the transverse mode, the electric field of a single Ag nanorod interacting with the neighbors is stronger than that of the Au substrate. In addition, the strongest enhancement is concentrated between the SNRs and graphene layer, revealing strong charge transfer between graphene and SNRs. As shown in Fig. 5(c), the longitudinal mode at 800 nm corresponds to dipole LSPR and the electric field enhancement occurs at the corners and neighbors of the SNRs, where the hot spots are pushed to the top corners of the SNRs, thus at the interface with the surrounding medium [38]. The maps corresponding to Fig. 5(a) to (c) show the evolution of the electric field amplitude when the wavelength of nanostructure increasing. At 300 nm, the enhancement factor of the electric field intensity around the nanostructure is weak. The zones of high near-field intensities are pushed to the left-top and left-bottom corners of the Au substrate. This is a consequence of the tip effect which accumulates charges in the corners of the Au substrate. When the wavelength increases to 800 nm, the amplitude is mostly uniform in this Au substrate and the polarization is perpendicular to the interface between graphene and SNRs. Within the silver nanorods, the polarization is linear and electric field lines flow from the graphene layer. This indicates that a strong charge effect occurs between graphene and SNRs and the surface charges are opposite between the left and the right edge of the nanostructure. This is consistent with the fact that the nanostructure behaves mostly like a dipole oriented along its long side at the LSP resonance. Hence, the study of the electric field distributions shows that within the peaks from 300 to 800 nm, the particle response evolves from mainly SPP to mainly LSP.

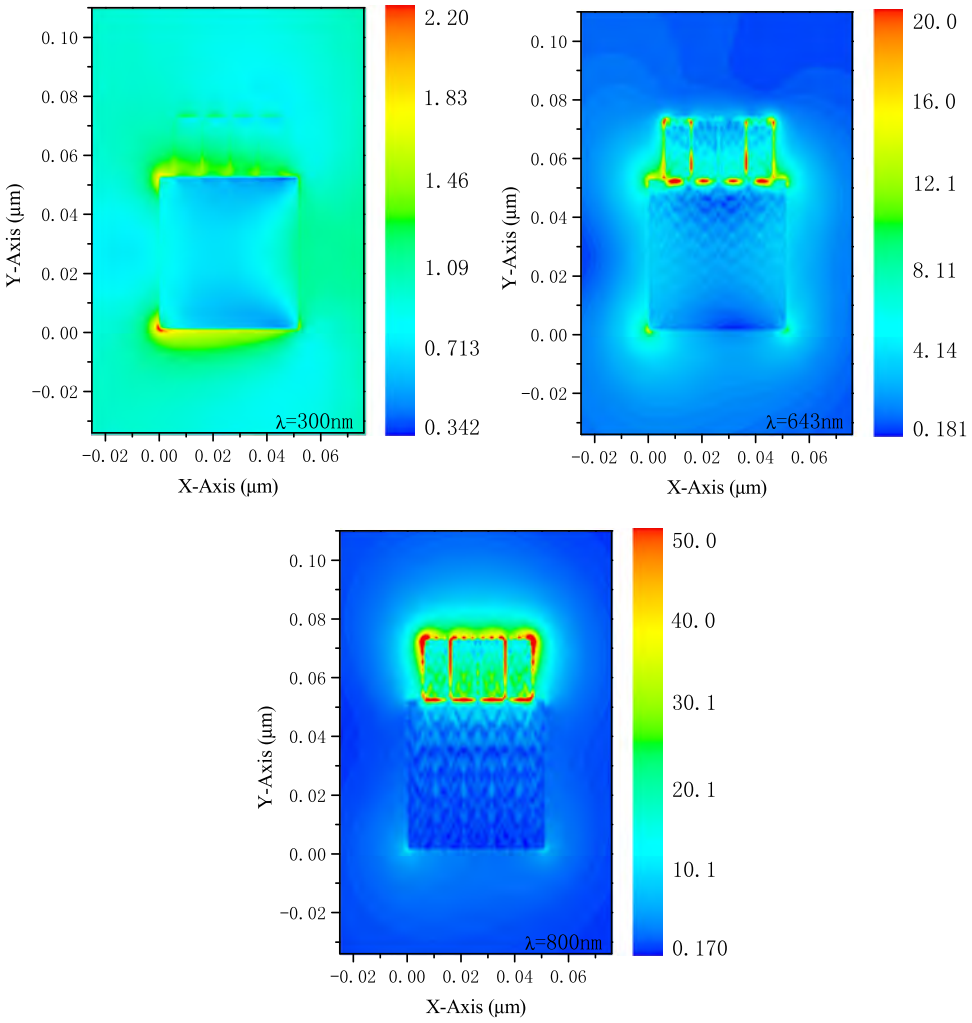

Fig. 5. Electric field enhancement contours around the SNRs/graphene/Au nanostructure illuminated at the plasmon resonance wavelength.

In order to investigate the influence of graphene layer on extinction efficiency, the extinction spectra of SNRs/graphene/Au nanostructure (20/1/50) and SNRs/Au nanostructure (20/50) without graphene layer are investigated, as shown in Fig. 6. It is seen that both nanostructures possess three resonance peaks and the resonance mode at $\lambda = 300$ nm has no significant shift, which means in-dependence on the graphene layer. The transverse mode at $\lambda = 630$ nm red-shifts as the thickness of the graphene layers increases from 0 to 1 nm. In the spectrum of SNRs/graphene/Au nanostructure, the intensity of the peak at 800 nm reaches a maximum, whereas the intensity of the peak at 860 nm in SNRs/Au nanostructure is much lower than the nanostructure with graphene layer. It can be concluded that the plasmon resonances of the SNRs/graphene/Au nanostructure are sensitive to the existence of graphene layer.

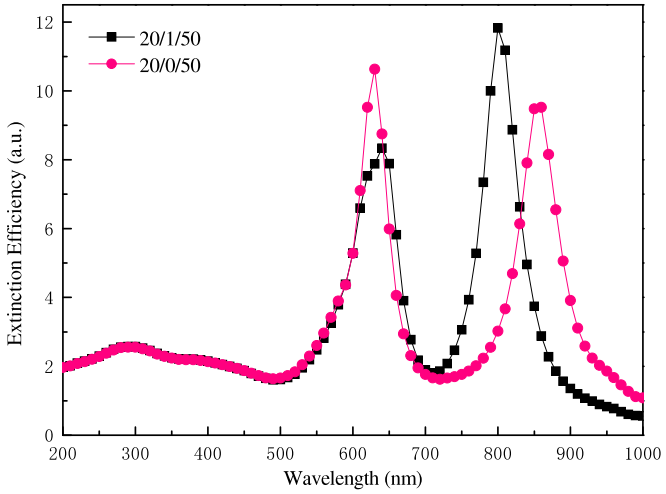

Fig. 6. Extinction spectra of the SNRs/graphene/Au nanostructure and SNRs/Au nanostructure. (For interpretation of the references to color in this figure legend, the reader is referred to the web version of this article.)

4. Conclusion

A systematic study is performed on the LSPR of SNR arrays deposited on the graphene-coated Au substrate by the DDA method. By calculating the LSPR extinction spectra and analyzing the corresponding electric field patterns at the resonance frequencies, graphene layer thickness, SNRs height, and refractive index of the surrounding medium are demonstrated to affect plasmon coupling and LSPR shifts. The simulation shows that the SNR array exhibits a complex plasmon hybridization behavior due to the interaction with the graphene-coated Au substrate. Three types of plasmonic modes with different resonance characteristics are localized on the SNRs/graphene/Au nanostructure. The blue-shift induced by different graphene layer thicknesses stem from charge transfer between the graphene layer and SNR array. Our results

indicate that the distinct plasmonic properties of the SNRs/graphene/Au nanostructure can be exploited in sensing applications.

Acknowledgments

This work was supported by the National Natural Science Foundation of China (Grant No. 51474069, 51374072), China Postdoctoral Science Foundation funded project (Grant No. 2016M591510), Natural Science Foundation of Heilongjiang Province (Grant No. E2016007), Graduate Innovation Project Of NEPU (Grant No. YJSCX2017-034NEPU), and City University of Hong Kong Applied Research Grant (ARG) No. 9667122.

References

[1] M. Rycenga, C.M. Cobley, J. Zeng, W. Li, C.H. Moran, Q. Zhang, D. Qin, Y. Xia, Controlling the synthesis and assembly of silver nanostructures for plasmonic applications, Chem. Rev. 111 (2011) 3669–3712.
[2] J. Chen, R.Q. Xu, Z.Q. Liu, C.J. Tang, Z. Chen, Z.L. Wang, Fabrication and infrared-transmission properties of monolayer hexagonal-close-packed metallic nanoshells, Opt. Commun. 297 (2013) 194–197.
[3] J. Wu, X. Lu, Q. Zhu, J. Zhao, Q. Shen, L. Zhan, W. Ni, Angle-resolved plasmonic properties of single gold nanorod dimers, Nano-Micro Lett. 6 (2014) 372–380.
[4] V.L.Y. Loke, G.M. Huda, E.U. Donev, V. Schmidt, J.T. Hastings, M.P. Menguč, T. Wriedt, Comparison between discrete dipole approximation and other modeling methods for the plasmonic response of gold nanosphere, Appl. Phys. B 115 (2014) 237–246.
[5] R. Takahata, S. Yamazoe, K. Koyasu, T. Tsukuda, Surface plasmon resonance in gold ultrathin nanorods and nanowires, J. Am. Chem. Soc. 136 (2014) 8489–8491.
[6] H.A. Atwater, A. Polman, Plasmonics for improved photovoltaic devices, Nature Mater. 9 (2010) 205–213.
[7] C.L. Haynes, A.D. McFarland, R.P. Van Duyne, Surface-enhanced Raman spectroscopy, Anal. Chem. 77 (2005) 338A–346A.
[8] V.G. Kravets, F. Schedin, A.V. Kabashin, A.N. Grigorenko, Sensitivity of collective plasmon modes of gold nanoresonators to local environment, Opt. Lett. 35 (2010) 956–958.
[9] Y. Gu, Q. Li, J. Xiao, K. Wu, G.P. Wang, Plasmonic metamaterials for ultrasensitive refractive index sensing at near infrared, J. Appl. Phys. 109 (2011) 023104-1–023104-6.
[10] J. Cesario, R. Quidant, G. Badenes, S. Enoch, Electromagnetic coupling between a metal nanoparticle grating and a metallic surface, Opt. Lett. 30 (2005) 3404–3406.
[11] J.J. Mock, R.T. Hill, A. Degiron, S. Zauscher, A. Chilkoti, D.R. Smith, Distance-dependent plasmon resonant coupling between a gold nanoparticle and gold film, Nano Lett. 8 (2008) 2245–2252.
[12] H. Chen, T. Ming, S. Zhang, Z. Jin, B. Yang, J. Wang, Effect of the dielectric properties of substrates on the scattering patterns of gold nanorods, ACS Nano 5 (2011) 4865–4877.
[13] R. Esteban, G. Aguirregabiria, A.G. Borisov, Y.M. Wang, P. Nordlander, G.W. Bryant, J. Aizpurua, The morphology of narrow gaps modifies the plasmonic response, ACS Photonics 2 (2015) 295–305.
[14] A. Geim, K. Novoselov, The rise of graphene, Nature Mater. 6 (2007) 183–191.
[15] H. Jussila, H. Yang, N. Granqvist, Z. Sun, Surface plasmon resonance for characterization of large-area atomic-layer graphene film, Optica 3 (2016) 151–158.
[16] F.H.L. Koppens, D.E. Chang, F.J. García de Abajo, Graphene plasmonics: A platform for strong light-matter interactions, Nano Lett. 11 (2011) 3370–3377.
[17] L. Wu, H.S. Chu, W.S. Koh, E.P. Li, Highly sensitive graphene biosensors based on surface plasmon resonance, Opt. Express 18 (2010) 14395–14400.
[18] A.C. Ferrari, F. Bonaccorso, V. Fal'Ko, K.S. Novoselov, S. Roche, P. Bøggild, S. Borini, F.H. Koppens, V. Palermo, N. Pugno, Science and technology roadmap for graphene, related two-dimensional crystals, and hybrid systems, Nanoscale 7 (2015) 4598–4810.
[19] B.T. Draine, P.J. Flatau, Discrete-dipole approximation for scattering calculations, J. Opt. Soc. Am. A 11 (1994) 1491–1499.
[20] D.E. Palik, Handbook of Optical Constants of Solids, Academic Press, New York, 1985.
[21] SOPRA N&K Database. www.refractiveindex.info.
[22] V. Kravets, A. Grigorenko, R. Nair, P. Blake, S. Anissimova, K. Novoselov, A. Geim, Spectroscopic ellipsometry of graphene and an exciton-shifted van hove peak in absorption, Phys. Rev. B: Condens. Matter Mater. Phys. 81 (2010) 155413-1–155413-6.
[23] A.L. Gonzalez, C. Noguez, G.P. Ortiz, Optical absorbance of colloidal suspensions of silver polyhedral nanoparticles, J. Phys. Chem. B 109 (2005) 17512–17517.
[24] M. Hasegawa, K. Nishidate, Transfer doping of a metallic carbon nanotube and graphene on metal surfaces, Phys. Rev. B 84 (2011) 1498–1504.
[25] M. Bokdam, P.A. Khomyakov, G. Brocks, P.J. Kelly, Field effect doping of graphene in metal|dielectric|graphene heterostructures: A model based upon first-principles calculations, Phys. Rev. B 87 (2013) 075414/1–075414/13.
[26] J. Granatier, P. Lazar, M. Otyepka, P. Hobza, The nature of the binding of Au, Ag, and Pd to Benzene, Coronene, and Graphene: From Benchmark CCSD(T) calculations to plane-wave DFT calculations, J. Chem. Theory Comput. 7 (2011) 3743–3755.
[27] P. Rani, G.S. Dubey, V.K. Jindal, DFT study of optical properties of pure and doped graphene, Physica E 62 (2014) 28–35.
[28] B.K. Kim, E.K. Jeon, J.J. Kim, J.O. Lee, Positioning of the Fermi level in graphene devices with asymmetric metal electrodes, J. Nanomater. 2010 (2010) 139–143.
[29] P. Nath, D. Sanyal, D. Jana, Optical properties of transition metal atom adsorbed graphene: a density functional theoretical calculation, Physica E 69 (2015) 306–315.
[30] M. Hu, A. Ghoshal, M. Marquez, P.G. Kik, Single particle spectroscopy study of metal-film-induced tuning of silver nanoparticle plasmon resonances, J. Phys. Chem. C 114 (2010) 7509–7514.
[31] P. Viste, J. Plain, R. Jaffiol, A. Vial, P.M. Adam, P. Royer, Enhancement and quenching regimes in metalsemiconductor hybrid optical nanosources, ACS Nano 4 (2010) 759–764.
[32] Y. Chu, K.B. Crozier, Experimental study of the interaction between localized and propagating surface plasmons, Opt. Lett. 34 (2009) 244–246.
[33] S. Link, M.A. El-Sayed, Size and temperature dependence of the plasmon absorption of colloidal gold nanoparticles, J. Phys. Chem. B 103 (1999) 4212–4217.
[34] P. Mao, J. Chen, R. Xu, G. Xie, Y. Liu, G. Gao, S. Wu, Self-assembled silver nanoparticles: correlation between structural and surface plasmon resonance properties, Appl. Phys. A 117 (2014) 1067–1073.
[35] J. Cesario, Electromagnetic coupling between a metal nanoparticle grating and a metallic surface, Opt. Lett. 30 (2005) 3404–3406.
[36] V.N. Rai, A.K. Srivastava, C. Mukherjee, S.K. Deb, Localized surface plasmon resonance and refractive index sensitivity of vacuum-evaporated nanostructured gold thin films, Indian J. Phys. 90 (2016) 1–10.
[37] G. Lévêque, O. J.F. Martin, Tunable composite nanoparticle for plasmonics, Opt. Lett. 31 (2006) 2750–2752.
[38] T. Maurer, R. Nicolas, G. Lévêque, P. Subramanian, J. Proust, J. Béal, S. Schuermans, J.P. Vilcot, Z. Herro, M. Kazan, J. Plain, R. Boukherroub, A. Akjouj, B. Djafari-Rouhani, P.M. Adam, S. Szunerits, Enhancing LSPR sensitivity of Au gratings through graphene coupling to Au film, Plasmonics 9 (2014) 507–512.